ACCOUNTS of chemical research

Article

pubs.acs.org/accounts

Electrocatalysis by Mass-Selected Pt_n Clusters

Published as part of the Accounts of Chemical Research special issue "Nanoelectrochemistry".

Alexander von Weber[†] and Scott L. Anderson*

Chemistry Department, University of Utah, 315 S. 1400 E., Salt Lake City, Utah 84112, United States

CONSPECTUS: Mass-selected Pt_n^+ ion deposition in ultrahigh vacuum (UHV) was used to prepare a series of size-selected electrodes with Pt_n ($n \leq 14$) clusters supported on either glassy carbon (GC) or indium tin oxide (ITO). After characterization of the physical properties of the electrodes in UHV, an *in situ* method was used to study electrocatalytic activity for the oxygen reduction and ethanol oxidation reactions, without significant air exposure. For each reaction studied, there are similarities between the catalytic properties of Pt_n-containing electrodes and those of nanoparticulate or bulk Pt electrodes, but there are also important differences that provide mechanistic insights. For all systems, strong cluster size effects were observed. For comparison, select experiments were done under identical conditions but with the Pt_n electrodes exposed to air prior to electrochemical studies, resulting in strong modification/suppression of catalytic activity due to adventitious contaminants.

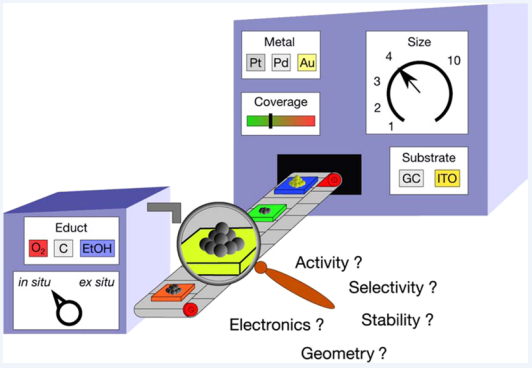

For ethanol oxidation at Pt_n/ITO, activity varies with size nonmonotonically, by more than an order of magnitude. The sharp size dependence persists during at least 30 to 40 cycles through the Pt redox potential, indicating that processes that would tend to broaden the size distribution are not efficient. All but the least active sizes are substantially more active *per* mass of Pt, than Pt nanoparticles under the same conditions. The oscillatory dependence of activity on size is anticorrelated with the binding energy of the Pt 4d core level, demonstrating that activity is controlled by the electronic structure of the supported clusters.

For oxygen reduction at Pt_n/ITO, the branching between water and hydrogen peroxide production is strongly dependent on cluster size, with small clusters selectively producing peroxide with high activity. The selectivity appears to be related to the size of the active site, with no obvious correlation to Pt electronic properties.

The most unusual effect seen was for Pt_n/GC, studied under acid conditions appropriate to oxygen reduction. Pt_7 and a few other cluster sizes show "normal" oxygen reduction activity, similar to what is measured for Pt nanoparticles on GC under the same conditions. Many of the small clusters, however, are found to catalyze highly efficient oxidation, by water, of the glassy carbon support, with essentially no overpotential. The high activity for carbon oxidation for many Pt_n/GC electrodes and the absence of significant carbon oxidation for a GC electrode with Pt nanoparticles raise the question of whether small Pt clusters may be responsible for much of the corrosion observed in Pt/carbon electrodes. This system provides another example where activity for oxidation catalysis is anticorrelated with the Pt core level binding energies, indicating that it is electronic, rather than geometric, structure that limits activity.

INTRODUCTION

We describe a series of experiments exploring the electrocatalytic activity of small, precisely size-selected Pt_n clusters on two different supports, prepared and characterized in ultrahigh vacuum (UHV), and studied *in situ* without significant air exposure. There are two motivations. From a fundamental perspective, the interest is in understanding how catalytic activity, selectivity, and stability relate to cluster size and to cluster−support interactions. Particularly for metal particles or clusters with sizes below a few nanometers, strong size effects are expected from both geometric and electronic considerations.[1−9] Properties such as average metal coordination and distributions of different types of binding sites are size dependent, as are metal electronic properties such as orbital energies or band gaps. In probing such effects, the ability to vary cluster size precisely, and independently of metal coverage, provides a useful mechanistic tool. For example, size-dependent correlations between catalyst activity and cluster physical properties give insight into which properties are most important in controlling activity.

From an applications perspective, one motivation is the need to reduce the precious metal content of catalysts. In typical nanoparticulate catalysts, most of the metal is in the bulk of the particles, where it cannot directly interact with reactants, while for small clusters, most or all of the metal is in the reactant-accessible surface layer. There is great current interest in "single atom catalysts", that is, catalysts where the support is designed to stabilize isolated atoms and small clusters of the catalytically active metal.[10−15] The challenge is to maintain or improve the

Received: July 25, 2016
Published: October 17, 2016

DOI: 10.1021/acs.accounts.6b00387
Acc. Chem. Res. 2016, 49, 2632−2639

activity and selectivity compared to nanoparticle catalysts, while making the isolated atoms/clusters stable in extended use. In addition to the expected electronic and geometric size effects on activity, the strong metal−support binding necessary to preserve dispersion under reaction conditions will also tend to perturb chemical properties, providing additional opportunities and challenges in tuning catalytic behavior. Experiments with size-selected clusters on relatively simple supports provide insights into the effects of both cluster size and cluster−support interactions.

We have been using size-selected cluster deposition to study catalytic reactions under surface science conditions for some time[6,7,16−20] and recently extended this approach to *in situ* studies of electrocatalytic oxygen reduction[8,21] and ethanol oxidation.[9] A number of groups have developed complementary capabilities for studying size-selected cluster-based electrodes, and their results are important in motivating and interpreting our work.[22−28] Our understanding has also benefited tremendously from the huge literature on oxygen reduction and alcohol oxidation, which space limitations preclude citing here.

METHODOLOGY FOR STUDYING SIZE-SELECTED ELECTRODES WITHOUT AIR EXPOSURE

Even brief air exposure leaves adsorbates on electrodes that can strongly modify their activities. Air-exposed electrodes can be cleaned by cycling them repeatedly through the surface redox potential; however, for electrodes with size-selected clusters, cycling could also affect the clusters. For example Hartl et al. showed that Pt clusters on carbon are stable at potentials below 0.55 V vs NHE, but not at potentials above ∼1 V.[22] To minimize complications from adsorbates, our experiment was designed to allow study of electrodes without air exposure.

The experiments are done in an ultrahigh vacuum (UHV) system that incorporates capabilities for cluster deposition, X-ray and UV photoelectron spectroscopy (XPS, UPS), ion scattering, and gas surface adsorption and reaction studies.[29] For electrochemistry, we attach an antechamber beneath the main chamber, housing a bakeable *in situ* electrochemical cell (Figure 1). The cell has three frit-separated compartments, two of which house a Pt mesh counter electrode and a Ag/AgCl reference electrode. The working compartment is open at one end, with an O-ring that seals to a cluster-containing electrode. Early experiments used a two-compartment cell, with working and counter electrodes sharing one compartment.

Laser vaporization in a pulsed helium flow is used to create cluster cations (here, Pt_n^+), which are mass selected and deposited at ∼1 eV/atom energy on UHV-cleaned glassy carbon (GC)[8] or indium tin oxide (ITO)[9] electrodes. Clusters are deposited in a 2 mm diameter spot, with typical coverage of 1.5×10^{14} Pt atoms/cm^2, ca. 10% of a Pt monolayer.

To start an electrochemical experiment, the antechamber and cell are evacuated and baked overnight. An electrode is cleaned in UHV, Pt_n clusters are deposited and characterized in UHV, and finally the electrode is inserted into the antechamber, which is then pressurized above 1 atm with ultrahigh purity argon. Syringes are used to pump electrolytes into the cell, while manipulators press the cell and working electrode together, sealing the cluster spot inside the working compartment. For the experiments described here, the working and counter electrode compartments were filled with 0.1 M $HClO_4$, and the reference compartment was filled with 0.1 M NaCl. For comparison, experiments were also run for polycrystalline Pt

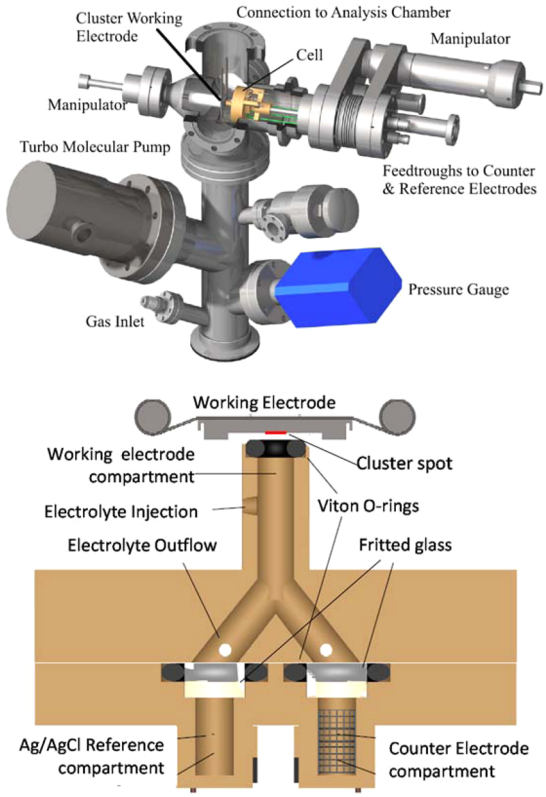

Figure 1. (top) Antechamber with cell. (bottom) Horizontal section of cell.

("Pt_{poly}") and for GC and ITO electrodes supporting Pt nanoparticles prepared by H_2PtCl_6 impregnation followed by reduction in H_2 ("Pt_{nano}").

Electrocatalysis was studied by running a series of cyclic voltammograms (CVs) under static electrolyte conditions. In all the CVs shown here, each cycle starts at the high potential limit, and CVs are plotted in terms of $\mu A/cm_{geo}^2$, where "geo" refers to the area of the 2 mm cluster spot. The potential ranges and numbers of CVs measured varied between the systems studied; however, in each case we first ran a few narrow range CVs where the lower potential limit was chosen to avoid H_2 generation, and the upper limit was well below the Pt_n redox potential. Subsequently, we ran a sequence of wider range CVs, covering the range between the onsets of the hydrogen and oxygen evolution reactions (HER and OER). Due to the small cell volume and small coverage of Pt_n (1.46 ng), Cl^- diffusing from the reference compartment started to poison the Pt_n after 15 to 20 min,[9] allowing only 30 to 40 CVs to be measured for each sample.

Note that for the low Pt coverages used in the size-selected Pt_n electrodes, the electrocatalytic currents observed are low enough that depletion of reactants (O_2, ethanol) from the electrolyte is negligible during the 30−40 CVs that could be run before Cl^- poisoning ended each experiment. Another important point is that for both the GC and ITO electrode substrates, control experiments were run in which clean, Pt-free electrodes were subjected to the identical sequence of CVs used to study the Pt_n/GC or Pt_n/ITO electrodes. These experiments showed only capacitive currents, with no evidence of catalytic activity or other currents developing during CV cycling. Finally, to allow direct comparison to the Pt_{nano} and control experiments, signals are reported as geometric current densities.

DOI: 10.1021/acs.accounts.6b00387
Acc. Chem. Res. 2016, 49, 2632−2639

In the Pt_n/GC experiments, current densities were calculated based on the wetted area on the electrode, which was essentially equal to the cluster spot area (~3.1 mm^2). A larger diameter cell was used in the Pt_n/ITO work, but the currents were again normalized to the cluster spot area. Because all experiments were done with 1.46 ng of Pt deposited, the current densities shown in the CVs can be converted to mass activities (current/gram Pt) by simply multiplying by 2.13×10^7.

An obvious question is whether this *in situ* procedure really results in clean electrodes. CVs for Pt_{poly} are sensitive to the presence of adventitious adsorbates, and in benchtop experiments, electrodes are cleaned by dozens of cycles through the metal redox potential. With our *in situ* procedure, we demonstrated that Pt_{poly} cleaned instead by UHV sputtering/annealing, gives CVs characteristic of clean Pt even on the first cycle.[8]

Low coverage Pt_n electrodes should be even more sensitive to contaminants, because of the smaller number of binding sites. There is no "clean" standard for Pt_n electrodes; however, under conditions appropriate to the oxygen reduction reaction (ORR), stable ORR currents are already present in the second CV on freshly introduced Pt_n/ITO or Pt_n/GC, even for CVs that stay well below the Pt redox potential. We conclude that our electrodes are quite clean, with any contaminants present removed during the first CV. The effects of deliberate air exposure are shown below.

SIMILARITIES TO Pt BULK OR NANOPARTICLE ELECTRODES

As noted, there are reasons to expect that electrocatalysis at small clusters might be qualitatively different from that at bulk or nanoparticle electrodes. In fact, however, there are many similarities. Figure 2 compares wide-range CVs for Pt_{nano}/GC

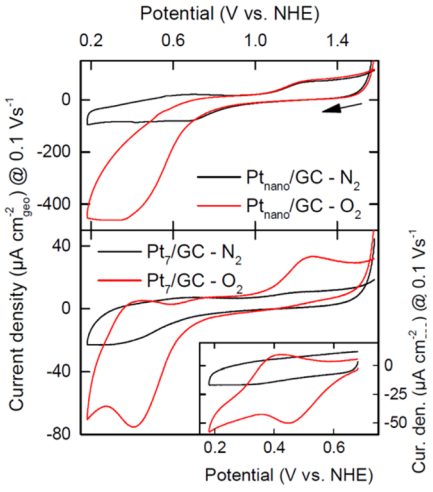

Figure 2. ORR CVs for Pt_{nano}/GC and Pt_7/GC.

in N_2- and O_2-saturated 0.1 M $HClO_4$, with analogous CVs for size-selected Pt_7/GC.[8] Potentials are given relative to the normal hydrogen electrode (NHE). The nanoparticles on the Pt_{nano} electrode were ~10 nm in diameter, with Pt loading of ~1 ML, roughly 10 times the Pt_7/GC coverage. The Pt_{nano}/GC sample, which was prepared on the benchtop, was cleaned by potential cycling before recording the CVs shown. Pt_7/GC was prepared in UHV and studied without air exposure. The first two CVs (narrow range) are shown in the inset (N_2, then O_2).

First consider the N_2-saturated CV for Pt_{nano}/GC. Positive current from OER is observed at the 1.58 V starting potential, and then between ~0.6 and 0.9 V, there is a negative current feature attributed to reduction of the initially oxidized Pt surfaces. In this example, the CV sweep was reversed before H^+ adsorption or HER would be expected. On the positive-going sweep, the feature between ~1.1 and 1.3 V results from reoxidation of the particle surfaces. The structure in the O_2-saturated CV for Pt_{nano}/GC is essentially identical at high potentials, but below 0.7 V, there is a large negative current feature from the ORR.

The narrow range CVs for Pt_7/GC (inset) show mostly capacitive current in N_2-saturated $HClO_4$, and a significant ORR feature in the O_2-saturated electrolyte. The wide range CVs for Pt_7/GC show structure similar to those for Pt_{nano}/GC, but with smaller currents, consistent with the ~10 times lower Pt loading. The ORR wave for Pt_7 has structure not seen for Pt_{nano}, presumably because there is no averaging over particle size. The main difference, however, is appearance of a distinct positive current feature peaking around 1.25 V in the O_2-saturated CV for Pt_7/GC. The fact that this peak is so much larger than in the N_2-saturated CV, points to some oxidation reaction that requires O_2, discussed below.

Figure 3 makes the same comparison between Pt_7 and Pt_{nano} deposited on ITO.[21] CVs are shown in both N_2- and O_2-

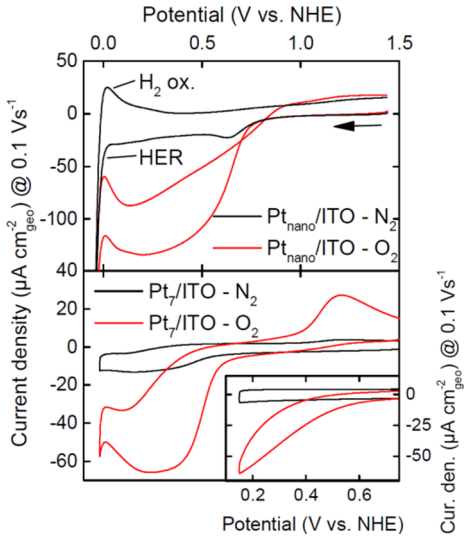

Figure 3. ORR CVs for Pt_{nano}/ITO and Pt_7/ITO.

saturated 0.1 M $HClO_4$. The Pt_{nano}/ITO CV shows structure similar to that seen for Pt_{nano}/GC, although here, the sweeps extended to lower potentials, allowing structure from HER and H_2 oxidation to be seen near 0 V. The bottom frame shows CVs for Pt_7/ITO. The qualitative structure is similar for Pt_7 and Pt_{nano}, apart from lower current for the lower coverage Pt_7. Again, however, Pt_7/ITO shows a large oxidation peak at ~1.25 V, not seen for Pt_{nano}/ITO. The ORR waves observed in the narrow and wide range CVs are similar, showing that ORR activity is not strongly affected by cycling through the Pt redox potential.

Finally, Figure 4 compares activity of Pt_{nano}/ITO and Pt_4/ITO for the ethanol oxidation reaction (EOR).[9] Pt_4 results are shown because Pt_7/ITO has low EOR activity. CVs were run in

DOI: 10.1021/acs.accounts.6b00387
Acc. Chem. Res. 2016, 49, 2632−2639

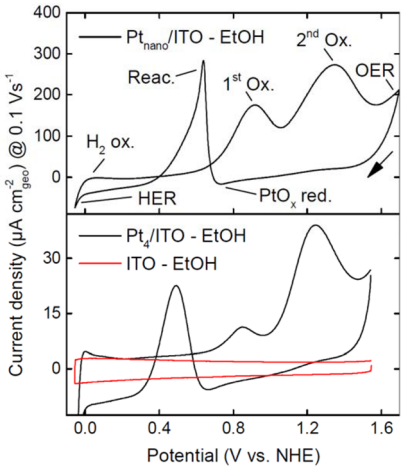

Figure 4. EOR CVs for Pt_{nano}/ITO and Pt_4/ITO.

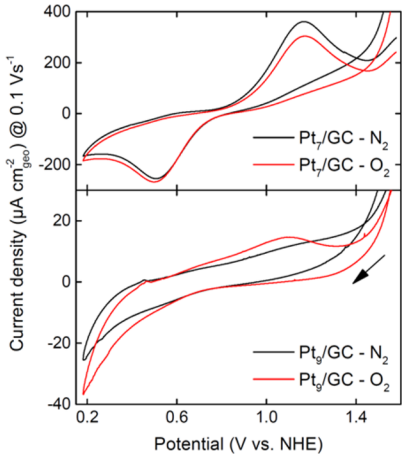

Figure 5. CVs for Pt_7/GC (top) and Pt_9/GC (bottom) after air exposure.

O_2-free 0.1 M $HClO_4$, to which either 1.0 or 2.0 vol % of ethanol was added for experiments with Pt_n/ITO and Pt_{nano}/ITO, respectively. The Pt_4/ITO sample had Pt loading of 0.1 ML, and the loading on Pt_{nano}/ITO was estimated to be ∼100 times higher, with mean particle size of ∼5 nm. The Pt_4 and Pt_{nano} current scales differ by a factor of 6.5. The lower frame also gives a CV for Pt-free ITO, showing only capacitive current with no EOR.

The CV structure for EOR is controlled by competition between oxidation reactions and electrode poisoning by products and intermediates. At the start of the negative-going sweep for Pt_{nano}/ITO, there is significant oxidation current due to OER, but then the current is small until the potential approaches ∼0.7 V, where a small negative current signals reduction of the initially oxidized Pt surface. Pt reduction enhances activity for ethanol oxidation, resulting in large positive current, but this "reactivation" feature quickly decays at lower potentials. As the potential drops below 0 V, the sharp onset of the HER is observed, and at that point, we reversed the sweep. On the positive-going sweep, there is a broad positive current feature near 0 V due to oxidation of H_2, and then activity is low until the potential reaches ∼0.8 V. The "1st oxidation" peak at ∼0.9 V has been shown by mass spectrometry to involve oxidation of adsorbed CO,[30] and there is a "2nd oxidation" peak near 1.25 V. Finally, the onset of OER can be seen near the end of the sweep. For the Pt_4/ITO sample, the potentials of the EOR peaks are shifted compared to those for Pt_{nano}/ITO, but the CV structure is strikingly similar.

In summary, for all three systems, the activity of Pt_n electrodes shows qualitative similarities to the activity observed for nanoparticulate or bulk Pt. The same reactions are observed, with current onsets and peaks at similar potentials. There are also important differences, but before discussing these, we first briefly show the effects of air exposure on the Pt_n activity.

COMPARISON TO AIR-EXPOSED ELECTRODES

A few experiments were run to test the effects of air exposure, following the procedure used above, but with the antechamber vented with air, rather than argon.[8] The top of Figure 5 shows CVs for air-exposed Pt_7/GC run under the same conditions used to study ORR in Figure 2. OER is seen at high potentials, but there is little evidence of ORR. Instead, there are peaks on the negative- and positive-going sweeps suggestive of redox reactions of some contaminant(s). In other examples (e.g., bottom frame), nearly featureless CVs were seen, again with weak ORR signal, indicating that the Pt_n were largely passivated by air contaminants. We tentatively attribute the run-to-run variability to differences in the contaminants present in the lab air when the antechamber was vented. We attempted to restore the activity of air-exposed electrodes by potential cycling, but for the ∼30 CVs we are able to run before Cl^- poisoning set it, cleaning was unsuccessful.

CLUSTER SIZE EFFECTS AND SIZE AS A MECHANISTIC TOOL

Under EOR conditions, the structure in CVs for different size Pt_n/ITO are similar to that shown in Figure 4 for Pt_4/ITO; however, the magnitudes of the EOR peaks are strongly size dependent, as summarized at the bottom of Figure 6. The peak currents for each cluster size were background corrected and converted to mass activities, that is, current per gram of Pt. It can be seen that the EOR mass activities vary with Pt_n size, by

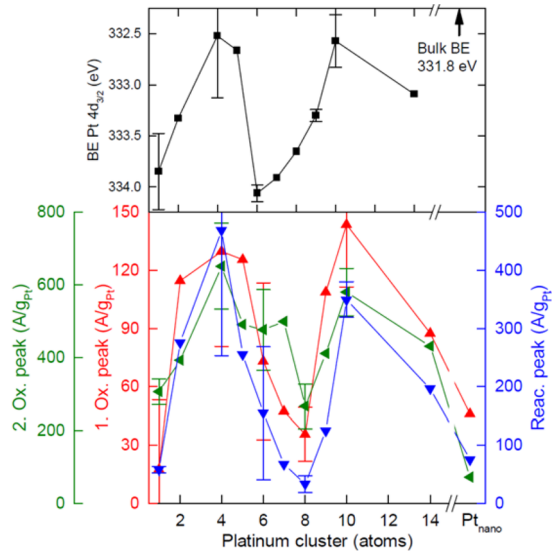

Figure 6. (top) Pt 4d BEs. (bottom) Mass activities for each EOR peak as a function of cluster size. Reproduced from ref 9 with permission from the PCCP Owner Societies.

DOI: 10.1021/acs.accounts.6b00387
Acc. Chem. Res. 2016, 49, 2632−2639

factors of between ~2.5 (2nd oxidation peak) and ~10 (reactivation peak), but that all three peaks have the same oscillatory dependence on cluster size. Activity maxima are seen at Pt_4 and Pt_{10} for all three EOR features, with minima at Pt_1 and Pt_8. The Pt_{nano}/ITO electrode had peak currents nearly an order of magnitude larger than that for Pt_4/ITO; however, the Pt loading was ~100 times higher, that is, the mass activities for all but the least active Pt_n/ITO are higher than those for Pt_{nano}/ITO, also shown in Figure 6. Higher mass activity is not surprising: most or all of the Pt is in the surface layer for small clusters.

One important point is that the size dependence is stable throughout the ~30–40 CVs we ran for each electrode, even though the clusters were cycled through their redox potentials. Because the size dependence is so strong and sharp, its persistence rules out significant sintering, dissolution, or other size-broadening processes during the set of CVs. The stability of Pt_n/ITO suggests strong Pt–substrate binding, and evidence to that effect is also found in the Pt 4d XPS binding energies (BEs) (top frame, Figure 6), as discussed below.

While the size-dependence remains sharp during potential cycling, the EOR currents do evolve, as shown in Figure 7 for

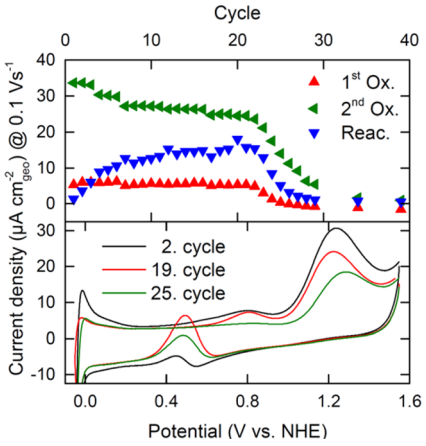

Figure 7. (top) Evolution of peak EOR currents during a sequence of CVs, for the 1st and 2nd oxidation and reactivation EOR peaks. (bottom) CVs measured at different points in the sequence.

the example of Pt_{10}. The top frame shows how the current density at the three EOR peaks varies during a sequence of CVs, and the bottom shows raw currents for the 2nd, 19th, and 25th CVs. The reactivation peak has near-zero initial intensity, increases sharply during the first ~10 cycles, and then changes slowly during the next dozen CVs, before being killed by Cl^- poisoning, which is complete by CV 30 in this example. In contrast, the second oxidation peak is at its maximum during the first CV for each Pt_n/ITO, decaying slowly during cycling, and the first oxidation peak is roughly independent of cycle number. The behavior is qualitatively similar for all cluster sizes studied, although the onset of Cl^- poisoning varied from CV 20 to 40, probably due to differences in injection of the NaCl reference electrolyte. The mass activities shown in Figure 6 are taken from CV 13 for each Pt_n/ITO, that is, just after the initial period of rapid evolution.

We can exclude potential-driven changes in cluster size as the origin of these current changes, because this would also broaden the size dependence, which is not observed. In addition, depletion of ethanol from the electrolyte should have been negligible. Therefore, the evolution of the EOR peaks is attributed to buildup of reaction products and intermediates on and near the electrodes.

In contrast to the strong size effect on EOR currents, the peak potentials are weakly affected by size. All three peaks are shifted to lower potentials compared to those for Pt_{nano}/ITO. Comparing Pt_4/ITO with Pt_{nano}/ITO, the shifts range from 65 mV for the first oxidation peak, to 150 mV for the reactivation peak. The variation in peak potentials for different Pt_n/ITO electrodes is smaller, only ~20 mV for the first oxidation peak and double that for the second oxidation and reactivation peaks. The second oxidation peak potential appears to be systematically higher for the less reactive Pt_n (n = 1, 8, 14), but otherwise there is no apparent pattern.

From a mechanistic perspective, perhaps the most interesting observation is that the EOR activity for each Pt_n/ITO is anticorrelated with the Pt $4d_{3/2}$ binding energy (BE) measured for the as-deposited electrode by XPS (the $4d_{3/2}$ peak was used because ITO interferes with the $4d_{5/2}$ peak). This anticorrelation is clear in Figure 6 (note inverted BE scale), and its implication is discussed below.

For ORR over Pt_n/ITO, the two main cluster size effects are summarized and compared to analogous results for Pt_{nano}/ITO in Figure 8. The ORR onset potentials are systematically size

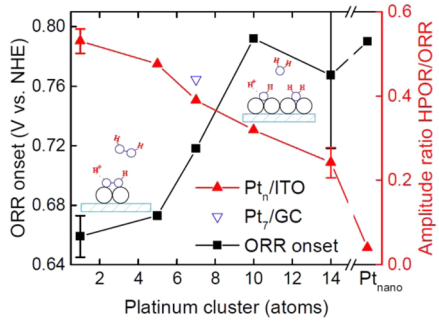

Figure 8. HPOR/ORR ratios and ORR onset potentials as a function of cluster size.

dependent. For Pt_{10}/ITO and Pt_{14}/ITO, the onset potentials are identical to that for Pt_{nano}/ITO, within experimental uncertainty, but for smaller clusters the onset potential decreases with decreasing size. Thus, the ORR overpotential increases with decreasing cluster size, exceeding that for Pt_{nano}/ITO by 130 mV for Pt_1/ITO.

The more dramatic cluster size effect relates to the oxidation peak seen at ~1.25 V on the positive-going sweep in O_2-saturated electrolyte (Figures 2 and 3). This feature is barely observable for Pt_{nano} but grows as cluster size decreases. There are two net ORR reactions:

$$O_2 + 4e^- + 4H^+ \rightarrow 2H_2O \quad \text{and}$$

$$O_2 + 2e^- + 2H^+ \rightarrow H_2O_2$$

The observed peak at 1.25 V is due to H_2O_2, formed by ORR at potentials below ~0.6 V, being catalytically oxidized back to O_2 as the potential is swept into the range where the Pt surface oxidizes:[31]

$$2Pt(OH) + H_2O_2 \rightarrow 2Pt(H_2O) + O_2$$

$$2Pt(H_2O) \rightarrow 2Pt(OH) + 2H^+ + 2e^-$$

DOI: 10.1021/acs.accounts.6b00387
Acc. Chem. Res. 2016, 49, 2632–2639

This hydrogen peroxide oxidation reaction (HPOR) is fast, and the HPOR current is limited by diffusion of H_2O_2 to the electrode,[31] that is, by the H_2O_2 concentration in the electrolyte. For our scan rate of 0.1 V/s, a significant fraction of the H_2O_2 remains near the electrode at the point where HPOR becomes possible; thus the HPOR/ORR current ratio, also plotted in Figure 8, is proportional to the H_2O_2 branching in ORR. The ratio varies from 0.04 for Pt_{nano}/ITO (similar to the value for Pt_{poly}) to 0.53 for Pt_1/ITO. We also include the ratio for Pt_7/GC, which is ~10% larger than the ratio for Pt_7/ITO. It might be thought that site blocking on the low coverage Pt_n/ITO electrodes might affect the H_2O_2 branching for the smallest clusters; however, the Pt coverage was identical in all Pt_n experiments.

In our experiment, we cannot directly measure the H_2O_2/H_2O branching in ORR; however, for 5 nm Pt particles supported on carbon in 1 M $HClO_4$, the H_2O_2 branching was reported to be ~20%.[32,33] If we assume that the branching under our conditions is even half that value for Pt_{nano}/ITO in 0.1 M $HClO_4$, then the implication would be that the H_2O_2 branching is near 100% for small clusters, such as Pt_1 and Pt_5.

The final size effect discussed here is by far the most dramatic that we have seen. Figures 2 and 3 show that Pt_7/GC has electrochemical properties similar to those for Pt_{nano}/GC or for Pt_7 or Pt_{nano} on ITO; however, this normal-looking behavior is actually anomalous. Figure 9 shows results for a more typical

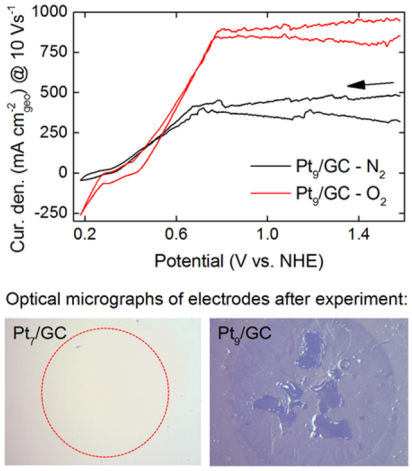

Figure 9. (top) ORR CVs for Pt_9/GC. (bottom) Postreaction images of the Pt_7/GC and Pt_9/GC electrodes.

cluster, Pt_9, and results for other cluster sizes are presented elsewhere.[8] CVs for Pt_9/GC in N_2- and O_2-saturated 0.1 M $HClO_4$ are shown in the top frame, covering the same potential range as in Figure 2 but scanned at 1 V/s, that is, 10 times faster than in Figure 2. There is signal suggestive of ORR at low potentials; however, for potentials above ~0.4 V, the currents are positive and >1000 times larger than any currents seen for Pt_7/GC or for any Pt_n/ITO (note mA, not μA). The "noise" on the current traces results from gas bubbles, and indeed, the reason these CVs were run at 1 V/s was that gas filled the cell and blocked current flow before a single CV could be completed at 0.1 V/s. Current could be restored by flushing gas out with fresh electrolyte but quickly decayed again.

The bottom frame of the figure compares optical micrographs of the Pt_7/GC electrode from the experiment in Figure 2 to the Pt_9/GC electrode used here. For Pt_9/GC, it is clear that extensive pitting occurred in the 2 mm diameter area where Pt_9 was deposited. The darkened circular area, where debris from the pitted area was deposited, corresponds to the ~3.5 mm wetted area in the cell. For Pt_7/GC (and also for Pt_{nano}/GC), there is no sign of electrode erosion in the cluster spot (red circle), even though the total time under reaction conditions was more than 100 times greater than for Pt_9/GC.

High oxidative currents, fast gas generation, and rapid electrode erosion indicate that Pt_9 efficiently catalyzes oxidation of the glassy carbon support. Pt_n/GCs in the n = 1−11 size range all showed somewhat different behavior, but rapid gas generation and electrode erosion were observed for all sizes except 7, 10, and 11. Similar behavior is seen in H_2SO_4 electrolyte. For the H^+ concentration used here, the possible carbon oxidation reactions are

$$CO_2 + 4H^+ + 4e^- \leftarrow C + 2H_2O$$

$$E^\circ = 0.28 \text{ V vs NHE}$$

$$CO + 2H^+ + 2e^- \leftarrow C + H_2O$$

$$E^\circ = 0.60 \text{ V vs NHE}$$

Our results show that most small Pt_n are able to catalyze carbon oxidation by water with high efficiency and low overpotential, raising the possibility that small Pt clusters may play an important role in carbon corrosion, a significant degradation mechanism for carbon-supported electrocatalysts.[34,35]

Figure 10 plots the Pt $4f_{7/2}$ BEs measured by XPS on the as-deposited Pt_n/GC samples. As expected from final state

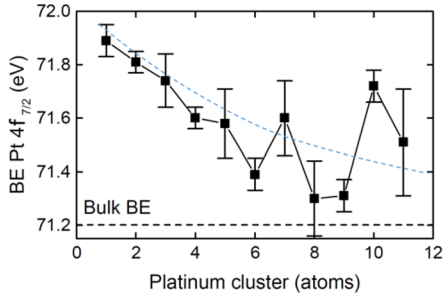

Figure 10. Pt $4f_{7/2}$ BEs for different Pt_n/GC electrodes. The dashed line is merely a guide for the eye.

screening considerations, the BEs are high for the small clusters, generally converging toward the bulk BE with increasing cluster size but with some oscillatory structure superimposed. The oscillations show that electronically, there can be substantial changes from adding or losing a single atom from the cluster. These electronic changes appear to be related to the very different electrochemical behavior seen for different size Pt_n/GC. Specifically, the only Pt_n that *do not* catalyze efficient carbon oxidation by water are Pt_7, Pt_{10}, and Pt_{11}, that is, just those Pt_n/GCs that have higher-than-trend 4f BEs. In other words, this is another example where core level BEs are anticorrelated with activity for oxidation catalysis.

CONCLUSIONS AND GENERAL OBSERVATIONS

For the three Pt_n electrocatalysis systems studied to date using our *in situ* method, there are several common threads. In each case, the CVs for at least some cluster sizes are qualitatively similar to those for bulk or Pt nanoparticle electrode; however,

DOI: 10.1021/acs.accounts.6b00387
Acc. Chem. Res. 2016, 49, 2632−2639

there are also strong effects of size on electrocatalytic activities, branching ratios, and onset or peak potentials.

For both oxidation reactions studied, size-dependent anticorrelations between Pt core level BEs and activity indicate that the electronic structure of the supported Pt_n has a major effect on activity. BEs for supported nanoparticles are often interpreted in terms of the effects of local electron density on the photoemission initial and final states. From either perspective, the anticorrelations suggest that the most active cluster sizes are more electron rich than average, and vice versa.[9] Recent high level theory for $Pd/SiO_2/Ru(0001)$[36] and for $Pd_n/TiO_2(110)$[37] has identified 4d−5sp hybridization as an important factor in shifting the 3d core level, and it is not unlikely that hybridization valence orbitals may also play a role for Pt_n. Clearly, changes in either electron density or hybridization can be expected to have catalytic consequences. We note that similar cluster size-dependent anticorrelations are seen between both core[6,20,38,39] and valence[7,20] electron BEs and CO oxidation activity under surface science conditions.

The other point to make regarding the core level BEs is that the size dependence is strongly affected by the support, as can be seen by comparing Figures 6 and 10. For GC, we were able to measure the BEs for the dominant Pt 4f peak, while for ITO, we measured Pt 4d BEs because the large In 4p signal from ITO overlaps the Pt 4f peaks. Nonetheless, it is clear that the oscillatory pattern of BEs is quite support dependent, indicating, not surprisingly, that interactions with carbon have quite different effects on Pt electron density/orbital hybridization than interactions with ITO. Furthermore, the shifts relative to the bulk BEs are much larger for Pt_n/ITO than for Pt_n/GC and show no sign of convergence to the bulk value. This behavior suggests that binding to ITO perturbs the Pt_n electronic structure more strongly than binding to GC, not surprising given the unreactive nature of glassy carbon.

For ORR, both onset potentials and H_2O_2/H_2O branching vary smoothly with cluster size (Figure 8), with no sign of any correlation to the strongly oscillatory XPS BEs (Figure 6), that is, electronic effects do not appear to be as important in this system. The fact that the HPOR/ORR ratio is similar for Pt_7/ITO and Pt_7/GC, despite the XPS results suggesting that their electronic properties are quite different, also tends to suggest that electronic effects are not rate-limiting. The obvious question is why small clusters, including Pt_1/ITO, give such high branching to H_2O_2. The cartoons shown in Figure 8 suggest one possibility. To produce H_2O, the Pt catalyst needs to provide sites where O_2 can dissociate, and one obvious hypothesis is that small clusters or isolated atoms simply do not have such sites. The H_2O_2/H_2O branching on small Pt_n and the extent to which it is influenced by geometric or electronic factors would appear to be an excellent target for theoretical analysis.

ORR branching to H_2O_2 is undesirable for energy applications; however, there is interest in selective H_2O_2 point-of-use electrosynthesis, thus avoiding the costs and hazards associated with transportation.[40] Our results suggest that isolated Pt atoms or small clusters, if they can be stabilized on electrode supports, would be a cost-effect approach to selected H_2O_2 production. Indeed, in the past six months, two papers have appeared reporting development of catalysts in which isolated Pt atoms and small clusters are stabilized on either titanium nitride[15] or sulfur-doped carbon supports.[14] As might be expected from the trend in Figure 8, these catalysts have high selectivity for H_2O_2 production.

In this Account, we have tried to illustrate both similarities and cluster size dependent differences between electrodes containing Pt atoms and small clusters, compared to electrodes with larger nanoparticles. In addition to being of practical interest from the perspective of "single atom catalysts", the ability to measure the effects of size on catalytic activity and correlate them to *in situ* spectroscopic measurements provides useful insights into which cluster properties are most important in controlling different types of reactions.

AUTHOR INFORMATION

Corresponding Author

*E-mail: anderson@chem.utah.edu. Phone: (801)585-7289.

Present Address

†A.v.W.: Technical University of Munich, Lichtenbergstraße 4, 85748 Garching, Germany/

Funding

This work was supported by the U.S. Department of Energy, Condensed Phase and Interfacial Molecular Science program, Grant No. DEFG03-99ER15003. A.v.W. was supported by a PROMOS scholarship from the Deutscher Akademischer Austauschdienst.

Notes

The authors declare no competing financial interest.

Biographies

Alexander von Weber is a Ph.D. student at Technical University of Munich and was a visiting scholar at the University of Utah as part of his physics M.S. from University of Konstanz in 2014. His interests include catalytic and optical properties of matter in the nonscalable size regime.

Scott L. Anderson is a Distinguished Professor of Chemistry at the University of Utah, with research interests in nanoparticle surface chemistry, catalysis, and combustion.

ACKNOWLEDGMENTS

Prof. Henry White provided essential advice on electrochemical technique, and Sebastian Proch, Mark Wirth, Michael Rosenfelder, Eric Baxter, and Matt Kane contributed to the experiments.

REFERENCES

(1) Tritsaris, G. A.; Greeley, J.; Rossmeisl, J.; Nørskov, J. K. Atomic-Scale Modeling of Particle Size Effects for the Oxygen Reduction Reaction on Pt. *Catal. Lett.* **2011**, *141*, 909−913.

(2) Alameddin, G.; Hunter, J.; Cameron, D.; Kappes, M. M. Electronic and geometric structure in silver clusters. *Chem. Phys. Lett.* **1992**, *192*, 122−128.

(3) Roy, H. V.; Fayet, P.; Patthey, F.; Schneider, W. D.; Delley, B.; Massobrio, C. Evolution of the electronic and geometric structure of size-selected Pt and Pd clusters on Ag(110) observed by photoemission. *Phys. Rev. B: Condens. Matter Mater. Phys.* **1994**, *49*, 5611−20.

(4) Campbell, C. T. Ultrathin metal films and particles on oxide surfaces: structural, electronic and chemisorptive properties. *Surf. Sci. Rep.* **1997**, *27*, 1−112.

(5) Freund, H.-J. Clusters and islands on oxides: from catalysis via electronics and magnetism to optics. *Surf. Sci.* **2002**, *500*, 271−299.

(6) Kaden, W. E.; Wu, T.; Kunkel, W. A.; Anderson, S. L. Electronic Structure Controls Reactivity of Size-Selected Pd Clusters Adsorbed on TiO_2 Surfaces. *Science* **2009**, *326*, 826−9.

DOI: 10.1021/acs.accounts.6b00387
Acc. Chem. Res. 2016, 49, 2632−2639

(7) Roberts, F. S.; Kane, M. D.; Baxter, E. T.; Anderson, S. L. Oxygen activation and CO oxidation over size-selected Ptn/alumina/Re(0001) model catalysts: correlations with valence electronic structure, physical structure, and binding sites. *Phys. Chem. Chem. Phys.* **2014**, *16*, 26443−26457.
(8) Proch, S.; Wirth, M.; White, H. S.; Anderson, S. L. Strong Effects of Cluster Size and Air Exposure on Oxygen Reduction and Carbon Oxidation Electrocatalysis by Size-Selected Pt_n ($n \leq 11$) on Glassy Carbon Electrodes. *J. Am. Chem. Soc.* **2013**, *135*, 3073−3086.
(9) von Weber, A.; Baxter, E. T.; Proch, S.; Kane, M. D.; Rosenfelder, M.; White, H. S.; Anderson, S. L. Size-Dependent Electronic Structure Controls Activity for Ethanol Electro-Oxidation at Pt_n/Indium Tin Oxide (n = 1 to 14). *Phys. Chem. Chem. Phys.* **2015**, *17*, 17601−17610.
(10) Yang, X.-F.; Wang, A.; Qiao, B.; Li, J.; Liu, J.; Zhang, T. Single-Atom Catalysts: A New Frontier in Heterogeneous Catalysis. *Acc. Chem. Res.* **2013**, *46*, 1740−1748.
(11) Flytzani-Stephanopoulos, M. Gold Atoms Stabilized on Various Supports Catalyze the Water-Gas Shift Reaction. *Acc. Chem. Res.* **2014**, *47*, 783−792.
(12) O'Mullane, A. P. From single crystal surfaces to single atoms: investigating active sites in electrocatalysis. *Nanoscale* **2014**, *6*, 4012−4026.
(13) Thomas, J. M. Catalysis: Tens of thousands of atoms replaced by one. *Nature (London, U. K.)* **2015**, *525*, 325−326.
(14) Choi, C. H.; Kim, M.; Kwon, H. C.; Cho, S. J.; Yun, S.; Kim, H.-T.; Mayrhofer, K. J. J.; Kim, H.; Choi, M. Tuning selectivity of electrochemical reactions by atomically dispersed platinum catalyst. *Nat. Commun.* **2016**, *7*, 10922.
(15) Yang, S.; Kim, J.; Tak, Y. J.; Soon, A.; Lee, H. Single-Atom Catalyst of Platinum Supported on Titanium Nitride for Selective Electrochemical Reactions. *Angew. Chem., Int. Ed.* **2016**, *55*, 2058−2062.
(16) Lee, S.; Fan, C.; Wu, T.; Anderson, S. L. CO Oxidation on Aun/TiO2 Catalysts Produced by Size-Selected Cluster Deposition. *J. Am. Chem. Soc.* **2004**, *126*, 5682−5683.
(17) Lee, S.; Fan, C.; Wu, T.; Anderson, S. L. Cluster size effects on CO oxidation activity, adsorbate affinity, and temporal behavior of model Aun/TiO2 catalysts. *J. Chem. Phys.* **2005**, *123*, 124710.
(18) Kaden, W. E.; Kunkel, W. A.; Kane, M. D.; Roberts, F. S.; Anderson, S. L. Size-Dependent Oxygen Activation Efficiency over Pdn/TiO2(110) for the CO Oxidation Reaction. *J. Am. Chem. Soc.* **2010**, *132*, 13097−13099.
(19) Kaden, W. E.; Kunkel, W. A.; Roberts, F. S.; Kane, M.; Anderson, S. L. CO adsorption and desorption on size-selected Pdn/TiO2(110) model catalysts: Size dependence of binding sites and energies, and support-mediated adsorption. *J. Chem. Phys.* **2012**, *136*, 204705.
(20) Kane, M. D.; Roberts, F. S.; Anderson, S. L. Effects of Alumina Thickness on CO Oxidation Activity over Pd_{20}/Alumina/Re(0001): Correlated Effects of Alumina Electronic Properties and Pd_{20} Geometry on Activity. *J. Phys. Chem. C* **2015**, *119*, 1359−1375.
(21) von Weber, A.; Baxter, E. T.; White, H. S.; Anderson, S. L. Cluster Size Controls Branching Between Water And Hydrogen Peroxide Production In Electrochemical Oxygen Reduction at Pt_n/ITO. *J. Phys. Chem. C* **2015**, *119*, 11160−11170.
(22) Hartl, K.; Nesselberger, M.; Mayrhofer, K. J. J.; Kunz, S.; Schweinberger, F. F.; Kwon, G. H.; Hanzlik, M.; Heiz, U.; Arenz, M. Electrochemically induced nanocluster migration. *Electrochim. Acta* **2010**, *56*, 810−816.
(23) Kunz, S.; Hartl, K.; Nesselberger, M.; Schweinberger, F. F.; Kwon, G.; Hanzlik, M.; Mayrhofer, K. J. J.; Heiz, U.; Arenz, M. Size-selected clusters as heterogeneous model catalysts under applied reaction conditions. *Phys. Chem. Chem. Phys.* **2010**, *12*, 10288−10291.
(24) Nesselberger, M.; Roefzaad, M.; Hamou, R. F.; Biedermann, P. U.; Schweinberger, F. F.; Kunz, S.; Schloegl, K.; Wiberg, G. K. H.; Ashton, S.; Heiz, U.; Mayrhofer, K. J. J.; Arenz, M. The effect of particle proximity on the oxygen reduction rate of size-selected platinum clusters. *Nat. Mater.* **2013**, *12*, 919−924.
(25) Lu, J.; Cheng, L.; Lau, K. C.; Tyo, E.; Luo, X.; Wen, J.; Miller, D.; Assary, R. S.; Wang, H.-H.; Redfern, P.; Wu, H.; Park, J.-B.; Sun, Y.-K.; Vajda, S.; Amine, K.; Curtiss, L. A. Effect of the size-selective silver clusters on lithium peroxide morphology in lithium−oxygen batteries. *Nat. Commun.* **2014**, *5*, 4895.
(26) Vajda, S.; White, M. G. Catalysis Applications of Size-Selected Cluster Deposition. *ACS Catal.* **2015**, *5*, 7152−7176.
(27) Zhou, W.-P.; Axnanda, S.; White, M. G.; Adzic, R. R.; Hrbek, J. Enhancement in Ethanol Electrooxidation by SnOx Nanoislands Grown on Pt(111): Effect of Metal Oxide-Metal Interface Sites. *J. Phys. Chem. C* **2011**, *115*, 16467−16473.
(28) Perez-Alonso, F. J.; McCarthy, D. N.; Nierhoff, A.; Hernandez-Fernandez, P.; Strebel, C.; Stephens, I. E. L.; Nielsen, J. H.; Chorkendorff, I. The Effect of Size on the Oxygen Electroreduction Activity of Mass-Selected Platinum Nanoparticles. *Angew. Chem., Int. Ed.* **2012**, *51*, 4641−4643.
(29) Kane, M. D.; Roberts, F. S.; Anderson, S. L. Mass-selected supported cluster catalysts: Size effects on CO oxidation activity, electronic structure, and thermal stability of Pd_n/alumina ($n \leq 30$) model catalysts. *Int. J. Mass Spectrom.* **2014**, *370*, 1−15.
(30) Wang, H.; Jusys, Z.; Behm, R. J. Ethanol Electrooxidation on a Carbon Supported Pt Catalyst: Reaction Kinetics and Product Yields. *J. Phys. Chem. B* **2004**, *108*, 19413−19424.
(31) Katsounaros, I.; Schneider, W. B.; Meier, J. C.; Benedikt, U.; Biedermann, P. U.; Auer, A. A.; Mayrhofer, K. J. J. Hydrogen peroxide electrochemistry on platinum: towards understanding the oxygen reduction reaction mechanism. *Phys. Chem. Chem. Phys.* **2012**, *14*, 7384−7391.
(32) Inaba, M.; Yamada, H.; Tokunaga, J.; Tasaka, A. Effect of agglomeration of pt/c catalyst on hydrogen peroxide formation. *Electrochem. Solid-State Lett.* **2004**, *7*, A474−A476.
(33) Inaba, M.; Yamada, H.; Tokunaga, J.; Tasaka, A. Size Effects of Platinum Nanoparticles on Activity, Peroxide Formation, and Durability of Pt/C Catalysts. *210th Electrochemical Society Meeting Abstracts*; Electrochemical Society: Pennington, NJ, 2006.
(34) Borup, R.; Meyers, J.; Pivovar, B.; Kim, Y. S.; Mukundan, R.; Garland, N.; Myers, D.; Wilson, M.; Garzon, F.; Wood, D.; Zelenay, P.; More, K.; Stroh, K.; Zawodzinski, T.; Boncella, J.; McGrath, J. E.; Inaba, M.; Miyatake, K.; Hori, M.; Ota, K.; Ogumi, Z.; Miyata, S.; Nishikata, A.; Siroma, Z.; Uchimoto, Y.; Yasuda, K.; Kimijima, K.-i.; Iwashita, N. Scientific Aspects of Polymer Electrolyte Fuel Cell Durability and Degradation. *Chem. Rev.* **2007**, *107*, 3904−3951.
(35) Meier, J. C.; Galeano, C.; Katsounaros, I.; Topalov, A. A.; Kostka, A.; Schüth, F.; Mayrhofer, K. J. J. Degradation Mechanisms of Pt/C Fuel Cell Catalysts under Simulated Start−Stop Conditions. *ACS Catal.* **2012**, *2*, 832−843.
(36) Kaden, W. E.; Büchner, C.; Lichtenstein, L.; Stuckenholz, S.; Ringleb, F.; Heyde, M.; Sterrer, M.; Freund, H.-J.; Giordano, L.; Pacchioni, G.; Nelin, C. J.; Bagus, P. S. Understanding Surface Core-Level Shifts using the Auger Parameter; a study of Pd atoms adsorbed on SiO2 ultra-thin films. *Phys. Rev. B: Condens. Matter Mater. Phys.* **2014**, *89*, 115436.
(37) Roberts, F. S.; Anderson, S. L.; Reber, A. C.; Khanna, S. N. Initial and Final State Effects in the Ultraviolet and X-ray Photoelectron Spectroscopy (UPS and XPS) of Size-Selected Pdn Clusters Supported on TiO2(110). *J. Phys. Chem. C* **2015**, *119*, 6033−6046.
(38) Wu, T.; Kaden, W. E.; Kunkel, W. A.; Anderson, S. L. Size-dependent oxidation of Pd_n ($n \leq 13$) on alumina/NiAl(110): Correlation with Pd core level binding energies. *Surf. Sci.* **2009**, *603*, 2764−2770.
(39) Kane, M. D.; Roberts, F. S.; Anderson, S. L. Alumina support and Pd_n cluster size effects on activity of Pd_n for catalytic oxidation of CO. *Faraday Discuss.* **2013**, *162*, 323−340.
(40) Verdaguer-Casadevall, A.; Deiana, D.; Karamad, M.; Siahrostami, S.; Malacrida, P.; Hansen, T. W.; Rossmeisl, J.; Chorkendorff, I.; Stephens, I. E. L. Trends in the Electrochemical Synthesis of H2O2: Enhancing Activity and Selectivity by Electrocatalytic Site Engineering. *Nano Lett.* **2014**, *14*, 1603−1608.

DOI: 10.1021/acs.accounts.6b00387
Acc. Chem. Res. 2016, 49, 2632−2639